



Rare earth element resources on Fuerteventura, Canary 1 Islands, Spain: a geochemical and mineralogical approach 2

3

Marc Campeny¹, Inmaculada Menéndez², Luis Quevedo^{2,3}, Jorge Yepes², Ramón 4 5 Casillas⁴, Agustina Ahijado⁴, Jorge Méndez-Ramos³, José Mangas²

6

7 ¹ Departament de Mineralogia, Museu de Ciències Naturals de Barcelona, Passeig Picasso s/n, 08003 Barcelona, Spain

, 8 9 ² Instituto de Oceanografía y Cambio Global, IOCAG, Universidad de Las Palmas de Gran Canaria, 35017 10 Las Palmas de Gran Canaria, Spain

³ Instituto de Materiales y Nanotecnología, Departamento de Física, Universidad de La Laguna, apartado 11

12 correos 456, 38200 La Laguna, Tenerife, Spain

13 14 ⁴ Departamento de Biología Animal, Edafología y Geología, Universidad de La Laguna, apartado correos

456, 38200 La Laguna, Tenerife, Spain.

15 16

17 Correspondence to: Marc Campeny (mcampenyc@bcn.cat)





18 Abstract. Rare earth elements (REEs) play a pivotal role in the ongoing energy and mobility transition 19 challenges. Given their critical importance, governments worldwide and especially from the European 20 21 22 23 24 25 26 27 28 29 30 31 32 33 34 Union, are actively promoting the exploration of REE resources. In this context, alkaline magmatic rocks (including trachytes, phonolites, syenites, melteigites and ijolites), carbonatites and their associated weathering products were subjected to a preliminary evaluation as potential targets for REE exploration on Fuerteventura Island (Canary Archipelago, Spain) based on mineralogical and geochemical studies. These lithologies show significant REE concentrations. However, only carbonatites exhibit the potential to host economically viable REE mineral deposits. REE concentrations in carbonatites of up to 10,301.83 ppm REY (REEs plus yttrium) have been detected, comparable to other locations hosting significant deposits of these critical elements worldwide. Conversely, alkaline magmatic rocks and the resulting weathering products display limited REE enrichment. Notably, REEs in carbonatites are associated with primary accessory phases such as REE-bearing pyrochlore and britholite, and secondary monazite. The carbonatites of Fuerteventura hold promise as prospective REE deposits within a non-conventional geological setting (oceanic island). However, due to intricate structural attributes and possible land use constraints, additional future detailed investigations are imperative to ascertain their genuine economic viability as substantial REE resources.

34 35

36 Keywords. Rare earth elements, Carbonatites, Fuerteventura, Canary Islands, Weathering





37 1 Introduction

38	The implementation of actions to mitigate climate change is one of the major global challenges facing
39	society today. In this regard, the European Commission (EC) has adopted a series of economic and
40	technological proposals aimed at reducing greenhouse gas emissions and transforming Europe into the first
41	climate-neutral continent by 2050. These guiding principles, encompassed in the European Green Deal
42	(EGD) (European Commission, 2019), are directly linked to the establishment of an energy and mobility
43	transition based on green technologies that will replace the current fossil fuel-based model. However, in
44	order to achieve the ambitious targets, other finite resources will be essential: metals. Some of them,
45	commonly referred to as green metals, will play a crucial role in a successful energy and mobility transition
46	and, consequently, in achieving the neutrality goals outlined by the EGD (Graedel et al., 2015; Jyothi et al.,
47	2020). Among the green metals is the group of rare earth elements (REEs) that are critical for a wide range
48	of high-tech applications such as wind turbines, electric vehicles, rechargeable batteries, energy-efficient
49	lighting, optical telecommunications, photovoltaic cells, solar energy harvesting or artificial photosynthesis
50	for "green hydrogen" (H ₂) generation (Méndez-Ramos et al., 2013; Acosta-Mora et al., 2018; Wondraczeck
51	et al, 2015). Such elements are also commonly known as the vitamins of modern industry (Alonso et al.,
52	2012; Chakhmouradian and Wall, 2012; Massari and Ruberti, 2013; Charalampides et al., 2015; Weng et
53	al., 2015; Balaram, 2019).
54	According to the International Union of Pure and Applied Chemistry (IUPAC), REEs comprise a group of
55	17 chemical elements: scandium (Sc), yttrium (Y) and the 15 members of the lanthanide series (Connelly
56	et al., 2005). The term "rare" is confusing because, even though REEs seldom occur in pure mineral phases,
57	their average concentration in the Earth's crust ranges from 150 to 220 ppm, surpassing other common
58	industrial metals such as copper, gold or platinum (Balaram et al., 2019; Long et al., 2010).
59	Given their pivotal role in modern industry and green technologies, as well as the projected increase in
60	demand for REEs in the coming years, governments worldwide are actively promoting the exploration of
61	new REE resources (Barteková and Kemp, 2016). In line with this, the EC included REE in the 2023 list
62	of critical raw materials (CRMs), acknowledging them as essential and considering heavy rare earth
63	elements (HREEs) as the material with the highest supply risk (European Commission, 2023a).
64	On March 16, 2023, the EC presented a bold initiative to the European Parliament: the "European Critical
65	Raw Materials Act". This regulation aims to establish a comprehensive framework to ensure a secure and

66 sustainable supply of CRMs, including REEs, in the coming years (European Commission, 2023b).





- 67 The search for REEs in the geological environment has primarily centred on investigating non-conventional 68 REE sources such as soils and weathering products (Braun et al., 1993; Wang et al., 2010, Wang et al., 69 2013; Berger et al., 2014; Aiglsperger et al., 2016; Torró et al., 2017; Reinhardt et al., 2018; Borst et al., 70 2020), but also traditional and well-known REE-bearing lithologies, such as carbonatites (Goodenough et 71 al., 2016; Yang et al., 2019; Pirajno and Yu, 2022). 72 Carbonatites are igneous rocks with a modal proportion of primary carbonates exceeding 50% (Le Maitre, 73 2002) and are genetically associated with a wide range of basic, ultrabasic, and alkaline silicate rocks. 74 Although carbonates such as calcite or dolomite are their main forming minerals, a significant portion of 75 carbonatites contain accessory phases enriched in critical metals such as REEs (Christy et al., 2021). REEs 76 can be contained in carbonates (e.g., bastnäsite, parisite, huanghoite, synchysite), phosphates (e.g., 77 monazite, rhabdophane), silicates (e.g., allanite), or even oxides (e.g., REE-bearing pyrochlore, cerianite). 78 These accessory minerals make carbonatites the main current REE source, representing 86.5% of the 79 deposits under exploitation for these elements (Liu et al., 2023). However, although carbonatites are rare 80 rocks, predominantly found in continental rifts associated with cratons (Humphreys-Williams et al., 2021), 81 they have exceptionally been described in other geological contexts, most notably oceanic islands 82 associated with hotspots, such as Cape Verde (Mourão et al., 2010; De Ignacio et al., 2018;) or 83 Fuerteventura in the Canary Islands (Mangas et al., 1996; Carnevale et al., 2021). 84 The petrogenesis of carbonatites is still a debated topic. Different processes have been proposed for their 85 formation, although there is a consensus that they originate from primary fusion processes derived from a 86 carbonated mantle (Kamenetsky et al., 2021). For the specific case of the oceanic carbonatites, this debate
- is even more lively. Doucelance et al. (2010) suggested a shallow origin from low-degree partial melting at the base of the oceanic lithosphere. Other authors have proposed the involvement of hydrothermal fluids of marine origin enriched in Ca that would have serpentinized the mantle (Park and Rye, 2013) or even the contribution of recycled marine carbonates through subduction or assimilated in shallow magma chambers

91 (Démeny et al., 1998; Hoernle et al., 2002; Doucelance et al., 2014).

92 Building on the aforementioned approach, the present work concentrates on the mineralogical and 93 geochemical study of carbonatites and associated alkaline igneous rocks, along with their weathering 94 products, in three different sectors in the western region of Fuerteventura (Canary Islands, Spain; Figure 95 1). The primary goal of this research is to conduct an initial evaluation of these materials, which are 96 genetically associated with a volcanic island linked to an oceanic intraplate magmatism. This assessment





- 97 aims to enhance our understanding of REE accumulation while appraising the potential of this peculiar
- 98 geological environment as a non-conventional source of REE.

- 100 2 Geological setting
- 101 2.1 The Canary Island Seamount Province
- 102 The Canary Islands archipelago, located between 27°N and 30°N of latitude, is part of the Canary Island
- 103 Seamount Province (CISP). This volcanic region forms a band of approximately 1300 km in length and
- 104 350 km in width, running parallel to the African continental margin. Within the CISP, there are over 100
- 105 seamounts and up to 8 emerged islands: El Hierro, La Palma, La Gomera, Tenerife, Gran Canaria,
- 106 Lanzarote, Fuerteventura and Savage islands (Courtillot et al., 2003; Schmincke and Sumita, 2010; van den
- 107 Bogaard, 2013). Based on magnetic anomaly measurements and dating of both emerged and submarine
- 108 igneous materials, volcanic activity in the CISP spans more than 142 Ma, from the Early Cretaceous to the
- 109 present day (Frisch, 2012; van den Bogaard, 2013; Longpré and Felpeto, 2021).





110 2.2 Fuerteventura Island

111	Fuerteventura, the easternmost island of the Canarian archipelago, along with Lanzarote, forms the
112	emergent crest of the Eastern Canarian Volcanic Ridge, which is located approximately 100 km offshore
113	from the Moroccan coast (Figure 1). Fuerteventura is the oldest island in the archipelago, with its initial
114	stages of formation linked with submarine volcanic activity, dating to the Oligocene (\sim 34 Ma). The first
115	episodes of subaerial volcanism occurred around ~23 Ma ago (Coello, 1992; Ancochea et al., 1996; Pérez-
116	Torrado et al., 2023).
117	Fuerteventura is characterized by the occurrence of three distinct main geological units, arranged in order
118	from oldest to youngest: the Fuerteventura basal complex (FBC), the Miocene subaerial volcanic units, and
119	the Pliocene-Quaternary volcano-sedimentary facies (Fúster et al., 1968; Le Bas et al., 1986; Muñoz et al.,
120	2005; Gutiérrez et al., 2006; Troll and Carracedo, 2016).

121

122 **2.2.1** The Fuerteventura basal complex

123 The unit of the FBC mainly outcrops in the western part of the island (Figure 1). Two different groups of 124 lithofacies may be distinguished: (1) Early Jurassic to Late Cretaceous oceanic crust materials (Steiner et 125 al., 1998), constituted by mid-ocean ridge basalts and oceanic sediments; (2) Oligocene submarine and 126 transitional volcanic rocks associated to plutonic bodies and dyke swarms (Feraud et al., 1985; Hobson et 127 al., 1998; Gutiérrez et al., 2006). In this second group, a set of lithologies can be distinguished related to 128 an ultra-alkaline-carbonatitic magmatic pulse that occurred ~25 Ma (Le Bas, 1981; Barrera et al., 1986; 129 Balogh et al., 1999). Additionally, alkaline ultramafic, mafic and felsic plutonic rocks such as wehrlites, 130 pyroxenites, gabbros and syenites intruded the previously existing Oligocene materials, forming distinctive 131 ring complexes. This intrusive activity led to processes of contact metamorphism, partial fusion and 132 metasomatism (Muñoz et al., 2005). These magmatic rocks, predominantly of Oligocene age, have been 133 interpreted as episodes of submarine and transitional growth in Fuerteventura (Le Bas et al., 1986; Gutiérrez 134 et al., 2006). 135 In general, outcrops related with the FBC intrusive assemblage exhibit significant variations and four 136 distinct morphologies and characteristic textures can be identified (Fúster et al., 1968; Barrera et al., 1986;

137 Le Bas et al., 1986; Fernández et al., 1997; Mangas et al., 1992, 1994, 1997; Ahijado 1999; Ancochea et

138 al., 2004; Ahijado et al., 2005; Muñoz et al., 2005):





139	(1) Dikes and veins of meter-scale, decimeter-scale, and centimeter-scale, that are randomly
140	distributed, resulting in a chaotic arrangement (Figure 2a, b). Related to the carbonatite veins and
141	dikes, an intense fenitization occurs.
142	(2) Shear zones (Fernández et al., 1997), characterized by gradual or diffuse boundaries, which
143	display assimilation structures between different rock bodies, along with the presence of
144	mylonites, and brecciated textures resulting from deformation (Figure 2c).
145	(3) Pegmatitic textures developed within certain rock bodies, often containing centimeter-sized
146	crystals of rock-forming minerals (Figure 2d).
147	(4) Contact metamorphism and metasomatism produced by late pyroxenite intrusions, as well as skarn
148	zones that occur in deformed or undeformed carbonatites, influenced by subsequent hydrothermal
149	fluid circulation (Ahijado et al., 2005; Casillas et al., 2008, 2011).
150	
151	In addition, during Miocene magmatic pulses, alkaline plutons were formed in the central-western part of
152	Fuerteventura Island north of the locality of Pájara (sector 2, Figure 1). These intrusions constitute typical
153	ring complexes of alkaline magmatic rocks, including nepheline syenites, syenites, and trachytes (Muñoz,
154	1969). They are regarded as the most recent rocks in the FBC (Figure 1) and have been dated using the K-
155	Ar method, yielding an approximate age of 20.6 ± 1.7 Ma (Le Bas et al., 1986; Holloway and Bussy, 2008).
156	
157	2.2.2 Miocene subaerial volcanic unit
158	During the Miocene, Fuerteventura witnessed the formation of up to three volcanic edifices (Figure 1;
159	Coello et al., 1992; Ancochea et al., 1996). The northern volcanic structure, referred to as the Tetir edifice,
160	experienced two volcanic construction phases between 22 and 12.8 Ma (Balcells et al., 1994). These
161	episodes involved the eruption of basalts, picritic basalts, oceanic basalts, trachybasalts and trachytes. In
162	the central part of the island, the Gran Tarajal edifice developed three different construction phases
163	spanning from 22.5 to 14.5 Ma (Balcells et al., 1994). On the Jandía Peninsula, in the southern part of the
164	island, a volcanic edifice comprising both basaltic and trachybasaltic materials emerged. It formed three
165	successive construction episodes occurring between 20.7 and 14.2 Ma ago (Balcells et al., 1994). Based on
166	their mineralogical and petrological features, the lithologies comprising this unit have not been considered
167	as potentially containing significant concentrations of REEs. Therefore, they have not been included in the
168	evaluation conducted in the present study.





170	2.2.3 Pliocene and Quaternary volcano-sedimentary facies
171	After the subaerial volcanic activity during the Miocene, a period of volcanic quiescence ensued, leading
172	to the erosion of the previously formed volcanic edifices. Subsequently, during the Pliocene (between 5.3
173	and 2.6 Ma), a phase of magmatic rejuvenation began, characterized by scattered Strombolian eruptions
174	(Figure 1). Concurrently, various sedimentary formations emerged across the entire island, including littoral
175	and shallow-water marine deposits, as well as aeolian, colluvial, and alluvial subaerial sediments and
176	paleosols from the Pliocene to the Quaternary (Fúster et al., 1968; Zazo et al., 2002; Ancochea et al., 2004).
177	The soils on Fuerteventura are predominantly classified as eutric cambisols and lithosols-vitric andosols,
178	according to the FAO/UNESCO (1970) nomenclature. However, the current arid and deforested conditions
179	have led to extensive erosion of the weathered rock profiles present in different areas of the island. Edaphic
180	calcretes are abundant in Fuerteventura (Alonso-Zarza and Silva, 2002; Huerta et al., 2015), with their
181	primary source of calcium believed to be the Pliocene paleodunes formed by calcarenites, rather than the
182	parent igneous rock itself (Chiquet et al., 1999; Huerta et al., 2015; Alonso-Zarza et al., 2020). Interestingly,
183	the aeolian dust deposits predominantly originate from the Sahara Desert (Goudie and Middleton, 2001;
184	Menéndez et al., 2007; Scheuvens et al., 2013).
185	
186	
187	
188	
189	3 Materials and Methods
190	3.1 Sampling
191	Alkaline magmatic rocks and, especially, carbonatites are considered potential targets for the exploration
192	of rare earth elements (Goodenough et al., 2016; Balaram et al., 2019; Beland and Jones, 2021). In
193	Fuerteventura, these types of lithologies are found in two distinct geological areas: the Oligocene (sectors
194	1 and 3; Figure 1) and the Miocene lithologies related with the FBC (sector 2, Figure 1).
195	Considering that weathering profiles may concentrate REE in larger quantities than primary bedrocks (Bao
196	and Zhao, 2008; Menéndez et al., 2019), these lithological formations were included in the present
197	evaluation study and sampling was conducted on a selection of six different profiles: (1) Agua Salada ravine





(sector 1) and (2) Aulagar ravine (sector 3), developed on carbonatites, (3) the FV-30 road, (4) Las Peñitas 199 quarry, (5) Palomares ravine and (6) the Pájara profiles, on syenite bedrock (Figure 1; Table S1). 200 Accordingly, a systematic sampling campaign was conducted in three different sectors of Fuerteventura, 201 targeting alkaline and carbonatitic igneous rocks and their associated weathering products. The specific 202 locations of these predetermined sectors are outlined in Figure 1. As a result, a set of 29 representative 203 samples of potentially REE-enriched magmatic rocks, along with 21 samples of associated weathering 204 products, were collected for further analysis and evaluation (Table S1). For the weathering products, we 205 conducted six sampling profiles (labelled A to F; Figure 1) at various suitable points to compare the 206 mineralogical and geochemical changes resulting from weathering of the primary magmatic rocks.

207

198

208 3.2 Petrographic and mineralogical studies

209 Selected samples of magmatic rocks were prepared in thin sections for textural and mineralogical analysis 210 at the Laboratory of Geological and Paleontological Preparation of the Natural Sciences Museum of 211 Barcelona (LPGiP-MCNB; Barcelona, Spain). A representative subset of these samples was also examined 212 using a JEOL JSM-7100 field emission scanning electron microscope (FE-SEM) at the Scientific and 213 Technological Centers of the Universitat de Barcelona (CCiTUB). The FE-SEM system is equipped with 214 an INCA Pentaflex EDS (energy dispersive spectroscopy) detector (Oxford Instruments, England), which 215 allowed for the acquisition of semi-quantitative analyses of mineral phases. The general operating 216 conditions for the FE-SEM were a 15-20 kV accelerating voltage and a 5 nA beam current.

217 To achieve accurate and precise mineralogical identification and characterization of the weathering 218 magmatic rocks and calcretes, X-ray powder diffraction (XRPD) measurements were performed using a 219 PANalytical Empyrean powder diffractometer equipped with a PIXcel1D Medipix 3 detector at the 220 Integrated XRD Service of the General Research Support Service of La Laguna University, Spain. The 221 diffractometer employed incident Cu K_{α} radiation at 45 kV and 40 mA, along with an RTMS (real-time 222 multiple strip) PIXcel1D detector with an amplitude of 3.3473° 20. The diffraction patterns were obtained 223 by scanning random powders in the 2θ range from 5° to 80°. Data sets were generated using a scan time of 224 57 seconds and a step size of 0.0263° (20), with a 1/16° divergence slit. Mineral identification and semi-225 quantitative results were obtained using the PANalytical's HighScore Plus search-match software (v. 4.5) 226 with a PDF+ database.





228 3.3 Geochemical analyses

- 229 The major elements composition of carbonates from carbonatites was studied using an electron probe
- 230 microanalyzer (EPMA) system. The EPMA analyses were conducted on a JEOL JXA-8230 electron
- 231 microprobe, equipped with five wavelength-dispersive spectrometers and a silicon-drift detector EDS,
- 232 located at the CCiTUB. The spot mode was employed for the analyses and the electron column was set to
- an accelerating voltage of 15 kV and a beam current of 10 nA. Standard counting times of 10 seconds were
- 234 used, along with a focused beam, to achieve the highest possible lateral resolution. The analytical standards
- 235 employed during the analysis process were: celestine (PETJ, Sr K_{α}) wollastonite (PETL, Ca K_{α}), periclase
- 236 (TAPH, Mg K_{α}), hematite (LiFH, Fe K_{α}), rhodonite (LiFH, Mn K_{α}) and albite (TAPH, Na K_{α}).
- 237 Bulk-rock geochemical data of major and trace element composition were obtained by X-ray fluorescence
- 238 (XRF) and inductive coupled plasma (ICP)-emission spectrometry. The samples were prepared by lithium
- 239 metaborate/tetraborate fusion and nitric acid digestion at the ACTLABS Activation Laboratories Ltd.
- 240 (Ancaster, Canada).
- 241

242 4 Results

243 4.1 Petrography and mineralogy

244 4.1.1 Alkaline magmatic rocks and carbonatites

245 The primary lithologies under study, consist of Oligocene (~25 Ma) alkaline igneous and carbonatitic rocks, 246 as well as Miocene alkaline lithologies (K-Ar age of 20.6±1.7 Ma; Le Bas et al., 1986), that form part of 247 the FBC. Their outcrops extend across kilometer-scale areas but exhibit high heterogeneity at a detailed 248 level due to the occurrence of numerous small intrusions, ranging in size from metric to decimetric 249 dimensions (Figs. 2a, b). 250 At a mineralogical level, separation of the different types of alkaline rocks found in the FBC is complex 251 because these lithologies are intimately associated and infiltrate diffusely, leading to the formation of hybrid 252 intrusions. The materials with the most basic composition correspond to pyroxenites and melteigites, and 253 their formation is associated with the earliest magmatic fractions. However, these are commonly spatially 254 associated with more differentiated rocks, mainly ijolites, nepheline syenites, and syenites. All these 255 lithologies have a relatively simple mineralogy, characterized by varying proportions of nepheline (10-30%

256 modal) and potassium feldspar (50-80% modal), associated with mafic minerals, primarily aegirine-augite





257 and biotite (10-30% modal). A set of accessory minerals with varying proportions (always less than 5% 258 modal) is also described, including ilmenite, titanite, zircon, and fluorapatite. 259 At a textural level, the alkaline series lithologies of the FBC present granular textures with millimeter-sized 260 euhedral grains. However, in some of the intrusions in sectors 2 and 3, pegmatitic syenites-ijolites were 261 detected with centimeter-sized grains characterized by the presence of large aegirine-augite crystals. 262 Some of the intrusions described in the three sectors show aphanitic textures caused by faster cooling, 263 resulting in rocks with similar mineralogy but extrusive-type textural characteristics. Therefore, due to their 264 textural features, some dikes and apophyses, although mineralogically equivalent, should be classified as 265 trachytes and phonolites. 266 Carbonatitic intrusions commonly co-occur with the alkaline rocks, sharing similar morphology, textures, 267 and spatial distribution within the outcrops (Figure 2e). Furthermore, alkaline and/or carbonatitic intrusions 268 can be occasionally associated with mafic intrusions, primarily pyroxenites and alkaline gabbros. In 269 addition, a subsequent set of mafic dikes with basaltic composition overlaps the previous intrusive bodies 270 (Figs. 2a, b). 271 All carbonatites described in different outcrops from sectors 1 and 3 are predominantly composed of calcite 272 (95% modal) and can thus be classified as calciocarbonatites (Le Maitre, 2005). None of the studied samples 273 shows the occurrence of ferromagnesian carbonates such as ankerite, dolomite, and/or siderite, as well as 274 REE carbonates. Texturally, calcite occurs as euhedral crystals ranging in size from millimetres to 275 centimetres, often recrystallized and exhibiting polysynthetic twinning. In some cases, a secondary micritic 276 calcite matrix is present, filling interstitial spaces and fractures. 277 The major element composition of calcite is relatively consistent across all the carbonatite samples. 278 Notably, there are significant contents of SrO, with values of up to 5.43 wt%, while REEs are absent from 279 the carbonate composition (Table S2). 280 The accessory mineralogy (~5% modal) comprises disseminated phases within the calcium carbonate. 281 Among them, the occurrence of minerals from the spinel group, including magnetite (Figure 3a), and 282 primarily jacobsite, occurring as subhedral crystals of up to 50 µm (Figure 3b). Another characteristic 283 mineral is perovskite, occurring as subhedral crystals of up to 100 µm. These grains are remarkable for 284 their significant Nb contents, as described in other carbonatitic localities worldwide (Torró et al., 2012). 285 Britholite also occurs as subhedral crystals of up to 100 µm (Figure 3b). This primary britholite contains 286 significant LREE content (Figure 4), and its alteration leads to the formation of secondary REE-enriched





- 287 phosphates, mainly monazite-Nd (Figure 3c), which also contains substantial amounts of La and Ce (Figure 288 4). REEs, in addition to occurring in primary britholite and secondary monazite, were also detected in tiny 289 pyrochlore grains, heterogeneously disseminated in the calcite groundmass (Figure 3b). In some cases, 290 pyrochlore forms euhedral crystals of up to 20 µm, also included in calcite (Figure 3d). This pyrochlore 291 shows slight zoning towards plumbopyrochlore (Christy and Atencio, 2013), with significant enrichment 292 in Pb observed at grain borders (Figure 3d). 293 Carbonatites can be affected by certain contact metamorphism, especially in sectors 1 and 3 (Figure 1) and 294 may exhibit a slightly different mineralogy from the one described thus far. This is characterized by the 295 occurrence of skarn-type metamorphic minerals, formed due to the interaction between carbonatites and 296 spatially associated silica-rich rocks. Among these minerals, there are subhedral crystals of andradite, up 297 to 30 µm in size, implanted in a matrix of secondary calcite and phlogopite, exhibiting pronounced zoning 298 with kerimasite cores (Figure 3e). In these areas, the occurrence of REE mineralizations associated with 299 allanite (Figure 3f) is also typical. Allanite occurs as granular aggregates associated with hydrothermal 300 secondary sulphates, primarily barite (Figure 3f), but occasionally celestine (Figure 3c).
- 301

302 4.1.2 Weathering products

303 In certain areas within the three studied sectors (Figure 1), there is evidence of the development of 304 characteristic shallow geological formations consistently associated with weathering, which affect the 305 outlined magmatic lithologies (Figs. 5, 6). These geological products were studied through the analysis of 306 six alteration profiles, developed on carbonatites (Agua Salada and Aulagar) and syenites (Palomares 307 ravine, FV-30 road, Las Peñitas quarry, and Pájara) (Figure 1).

308 The weathering products observed in the carbonatite profiles generally consist of centimetre-scale calcrete 309 veins injected into the bedrock, seemingly without any apparent connection to the current upward lithosol 310 (Figure 5). In general, apart from these calcrete horizons, the development of soils or other weathering 311 products was not detected on carbonatites in any of the studied sectors of the FBC. 312 Weathering products developed on syenite bedrock are generally more abundant, and the corresponding

alteration profiles are better preserved than in carbonatites. The cambic B horizon displays reddish to
yellowish colorations (5YR6/6), with a thickness of up to 20-30 cm. Additionally, it is common to find BC

- 315 horizons instead of B horizons, while the C horizon is well-developed, reaching a 30-40 cm thickness at
- 316 certain levels of the profile (Figure 6). Furthermore, except for the Las Peñitas profile (E profile, Figure 1),





- 317 centimetre-scale calcrete bands (Bk; Jahn et al., 2006) were also detected in deeper layers across all the
- 318 studied profiles.
- 319 In terms of mineralogical composition, carbonatite profiles exhibit significant changes due to weathering.
- 320 In general, weathering processes lead to a reduction in calcite and illite/chlorite, the disappearance of
- 321 fluorapatite, and the formation of secondary minerals like palygorskite (Figure 7). The contribution from
- 322 lateral slope movement is also evident through the presence of residual plagioclase and clinopyroxene.
- 323 In the case of syenite weathering profiles, illite/chlorite and kaolinite are the predominant secondary
- 324 products, followed by muscovite and palygorskite (Figure 7). Other minerals such as quartz were also
- 325 detected, even in the C horizons.
- 326

327 4.2 Bulk-rock and mineral geochemistry

- 328 Chemical analysis of the major, minor and trace elements were carried out in order to evaluate the
- 329 distribution of critical elements, especially REEs, on 25 representative samples of igneous rocks from the
- 330 FBC, including trachytes, phonolites, syenites, ijolites and carbonatites (Table S3). In addition, we also
- analysed 21 samples of weathering products (Table S4).

The total REY (REEs plus yttrium) content in the FBC igneous rocks exhibits widespread and significant enrichment in comparison to the average crustal values (150 to 220 ppm, Balaram et al., 2019). Notably, the extrusive and magmatic alkaline lithologies (trachytes and phonolites as well as syenites and ijolites) show variable REY values ranging between 230.63 and 1401.54 ppm (Table S3). In contrast, the

- 336 carbonatitic rocks exhibit REY content more than ten times greater than the alkaline lithologies, with
- 337 specific samples reaching maximum values of up to 10,301.83 ppm, as evidenced in sample 85a sourced
- 338 from a carbonatite outcrop in sector 1 (Table S3).

The weathered magmatic rocks, though moderately significant in REY content relative to the average crustal values (Table S4), still exhibit slightly lower levels compared to the content observed in the associated alkaline and carbonatitic protoliths (Table S3). A contrasting pattern emerges in the calcretes, where REY values experience a sharp reduction, presenting virtually negligible values ranging between 20.09 and 72.37 ppm REY. These levels are significantly below the average Earth's crust values (Balaram et al., 2019) and are markedly lower than those observed in both the alkaline lithologies and, particularly,

the carbonatites of the FBC.





346	REE normalized diagrams further underscore this distribution, portraying elevated content in the
347	carbonatites, followed by the alkaline rocks (Figure 8a). Meanwhile, the weathered magmatic rocks and
348	calcretes (Figure 8b) display significantly lower values. All studied lithologies exhibit clear negative
349	patterns, indicative of enrichment in light rare earth elements (LREEs) relative to HREEs. Notably,
350	carbonatites and alkaline rocks (Figure 8a) exhibit a flattening of these negative patterns in the final
351	segment, indicating a certain degree of HREE enrichment.
352	Importantly, the present study does not reveal significant contents of other critical minor and trace elements
353	in any of the examined lithologies. In fact, the FCB carbonatites exhibit a depletion in some critical
354	elements commonly associated with this lithology such as Nb or Ta (Table S3). Negative anomalies of both
355	Nb and Ta are clearly observed in the multi-element diagrams of carbonatite samples (Figure 9a).
356	Additionally, alkaline rock patterns also show a distinctive negative anomaly in Sr (Figure 9b). As for the
357	weathering products, their contents of other minor elements do not indicate significant concentrations of
358	metals or critical elements like Nb or Ta (Table S4). The multi-element diagrams for the calcretes exhibit
359	a negative Ta anomaly (Figure 9c), while the patterns of weathered magmatic rocks do not reveal notable
360	anomalies in any group of elements (Figure 9d).
361	A specific geochemical study of REE distribution in the six studied weathering profiles was also conducted
362	(Figure 10). The main objective was to evaluate the geochemical interactions between the protolith and the
363	related weathering lithologies, with the aim of detecting potential REE enrichments or depletions caused
364	by weathering processes.
365	In the exchange patterns of calcretes associated with carbonatitic protoliths, as analyzed in the Agua Salada
366	and Aulagar ravine profiles (Figs. 10A, B), REE concentrations are two orders of magnitude lower than in
367	the carbonatite (Figure 10A), as also previously determined from the REE diagrams (Figure 8). Notably, it
368	was found that the REE concentration is directly proportional to the distance from the protolith (Figure
369	10B), and calcrete samples with the highest REE concentrations (sample 14; Figure 10) were found in
370	closer proximity to the primary carbonatites than more REE depleted samples (samples 15 and 18; Figure
371	10B). In addition, although the values of all elements are depleted in the calcrete patterns, there is a greater
372	depression in LREE than in HREE relative to the protolith, resulting in typically positive patterns, except
373	for sample 76 from the Agua Salada ravine, where a clear inverse trend is observed (Figure 10A).
374	In general, the diagrams in Figure 10 show that weathering products on syenites exhibit enrichment relative
275	to the most life (many energy in Figs 10C, D, F). However, extends even by whether derived from

375 to the protolith (green areas in Figs. 10C, D, E). However, calcrete samples, whether derived from





- carbonatites or syenites, consistently show depletions compared to the protolith contents (reddish areas in
 Figs. 10C, D, F). The diagrams corresponding to the weathering products generated on syenites exhibit
 similar morphologies (Figs. 10C, D, E, F). Overall, these lithologies are characterized by enrichment in
 REEs relative to the protolith as well as V-shaped patterns, featured by the presence of a negative anomaly
- 380 in Eu, which is also reported in all C and B horizons developed on syenites, except sample 61 (Figure 10C),
- 381 and is likely related to plagioclase crystallization.
- 382

383 5 Discussion

384 5.1 REE evaluation of the FBC magmatic rocks

385 The FBC magmatic rocks, in the three study sectors, encompass alkaline lithologies (trachytes, phonolites, 386 syenites, melteigites, and ijolites) as well as carbonatites. Regarding the group of alkaline rocks, the 387 detected REE content varies between 214.1 and 1330.8 ppm (Table S3), significantly higher than the 388 average concentration determined in the Earth's crust (150 to 220 ppm; Balaram et al., 2019). However, 389 this finding is not surprising, and the observed values in Fuerteventura are not anomalous, as these types of 390 lithologies typically exhibit REE concentrations within this range (Dostal, 2017). Therefore, the measured 391 REE concentrations are neither significant nor sufficiently elevated to hypothetically consider these 392 lithologies as a potential non-conventional deposit of these critical elements in the FBC.

393 On the other hand, FBC carbonatites present significantly higher values in terms of REE content. In the 394 studied carbonatite samples from sectors 1 and 3 (carbonatites do not outcrop in sector 2), REE content 395 ranges between 1315.4 ppm and 10144.1 ppm. The latter value corresponds to the richest REE-detected 396 sample in the entire FBC, which is located in the Agua Salada ravine area of sector 1 (Table S3; Figure 1). 397 The reported REE content values in the FBC carbonatites are similar to the general average concentrations 398 found in other locations worldwide where carbonatites are exploited for REE extraction. This is the case, 399 for example, of Bayan Obo, the largest REE mine in the world in terms of reserves and production (Lai et 400 al., 2015; Liu et al., 2018). In this locality, high-grade carbonatites exhibit average concentrations of 2880 401 ppm (Wu et al., 2008; Smith et al., 2015, 2016), which are equivalent to those measured in some of the 402 samples from Fuerteventura. It should be noted that low-grade carbonatite ore from Bayan Obo presents 403 extremely high values in comparison to the FBC, with REE concentrations reaching 30,750 ppm (Chao et 404 al., 1997; Smith et al., 2016).





405	Another significant example is the Mountain Pass carbonatite in California, USA, regarded as the largest
406	REE mine in the American continent, intermittently in operation for REE extraction since 1954 (Olson et
407	al., 1954; Haxel, 2005). In this REE deposit, average value across the whole complex are around 2581 ppm
408	(Castor et al., 2008; Mariano and Mariano, 2012; Smith et al., 2016), also in line with REE concentrations
409	detected in the present study for the FBC carbonatites.
410	This comparative analysis can also be carried out using normalized REE values (Figure 11). In this regard,
411	FBC carbonatites are significantly depleted in LREE compared to those from Bayan Obo (Yang et al.,
412	2019) and Mountain Pass (Castor et al., 2008), although they show similar values to other REE deposits
413	associated with carbonatites, such as those in Ashram, Canada (Beland and Jones, 2021) and Bear Lodge,
414	USA (Moore et al., 2015; Smith et al., 2016; Figure 11) However, the pattern of the Fuerteventura
415	carbonatites exhibits a slightly less pronounced slope, indicating a higher relative content of HREE, which
416	are considered the materials with the highest risk of supply among all the CRMs defined by the EC
417	(European Commission, 2023a). In fact, in the FBC carbonatites, the normalized HREE values are
418	equivalent to those reported in the primary carbonatitic rocks from the deposits of Bayan Obo (China) and
419	Mountain Pass (USA) (Figure 11). The relative significant HREE content reported in FBC carbonatites
420	holds particular significance for several economic and technological reasons. The use of HREEs, such as
421	Yb, Er, and Tm, is of particular interest in cutting-edge photonic and nanotechnology applications.
422	However, HREEs can also play a pivotal role in addressing the market equilibrium challenge, as explained
423	by Falconnet (1985) and Binnemans et al. (2013). The overarching idea is to mitigate surpluses of specific
424	metals that could potentially disrupt market stability due to varying REE abundance ratios. This market
425	equilibrium issue compels industries to seek new applications for less commonly utilized HREEs that tend
426	to accumulate in the manufacturing processes. Consequently, this approach can help reduce the overall
427	price of all REEs, as production costs are distributed among all the elements.
428	At the mineralogical level, it was observed that, in the FBC carbonatites, the main REE-hosting minerals
429	are accessory phases; primarily minerals from the pyrochlore group, found as disseminated euhedral micro-
430	crystals implanted in primary calcite (Figs. 3b, d). Another REE-bearing mineral in the FBC carbonatites
431	is britholite, which exhibits significant LREE content. However, this mineral is commonly altered to
432	monazite (Figs. 3c, 4), interpreted as a secondary phase but also a carrier of these critical elements (Chen
433	et al., 2017).





- 434 Another noteworthy aspect is that the magmatic carbonate forming the FBC carbonatites is predominantly 435 calcite. REE carbonates like bastnäsite REE(CO3)F, parisite Ca(REE)2(CO3)3F2, synchysite 436 Ca(REE)(CO₃)₂F or huanghoite Ba(REE)(CO₃)₂F, do not occur in the FBC, as they do in other REE 437 deposits associated with, for example, the Bayan Obo carbonatite or the Sulphide Queen carbonatite from 438 Mountain Pass (Castor et al., 2008; Smith et al., 2015, 2016). This point is crucial for a future hypothetical 439 evaluation of the FBC carbonatites, as the processing of oxides and phosphates for REE extraction is a 440 much more complex and expensive treatment process than for REE-bearing carbonates (McNulty et al., 441 2022).
- 442

443 5.2 REE evaluation of associated weathering products

444 The weathering materials developed on magmatic rocks, also analysed for their REE concentrations, 445 constitute the remnants of soils that were interpreted as developed under wetter conditions during a humid 446 phase of the oxygen isotope stage 2, spanning from 29 to 20 thousand years BP (Huerta et al., 2016). This 447 period aligns with the last glacial maximum, marked by heightened humidity in the Canary Islands, 448 resulting in slope erosion and the formation of talus flatiron (Gutiérrez-Elorza et al., 2013). Over time, these 449 materials have undergone substantial volume reduction due to human-driven deforestation and erosion, 450 primarily before the 15th century (Machado-Yanes, 1996). Notably, topography plays an essential role in 451 the distribution of these weathering profiles and influences specific physical attributes such as slope 452 (FAO/UNESCO, 1974).

453 The studied weathering products developed on syenite rocks (profiles C, D, E, F; Figs. 1, 7) are classified 454 by FAO/UNESCO (1974) as eutric cambisols, reflecting a Mediterranean climate condition. Indeed, on the 455 African continent, which is adjacent to the Canary Islands, eutric cambisols are primarily found within the 456 tropical subhumid zone, gradually transitioning into the semi-arid zone (FAO/UNESCO, 1974). These 457 syenite weathering profiles exhibit better-preserved characteristics and a more significant extent compared 458 to those studied in carbonatites (profiles A and B; Figs. 1, 7). In general, intensive weathering plays a 459 crucial role in the formation of REE deposits, as these elements tend to be concentrated in such geological 460 formations compared to others leached during the weathering process. This phenomenon is exemplified in 461 several locations worldwide, where REE deposits associated with weathering products are also actively 462 exploited: for instance, Bear Lodge in the USA (Andersen et al., 2017), Chuktukon and Tomtor in Russia 463 (Kravchenko and Pokrovsky, 1995; Kravchenko et al., 2003; Chebotarev et al., 2017), Las Mercedes in the





464	Dominican Republic (Torró et al., 2017), Araxá in Brazil (Braga and Biondi, 2023), and Mount Weld in
465	Australia (Zhukova et al., 2021), among many others. However, the weathering processes on Fuerteventura
466	are characterized by fluctuating climatic conditions and intense erosion in the context of a typical
467	Mediterranean climate, which is in turn characterized by drier conditions and a lower propensity for intense
468	weathering compared to tropical climates. The weathering processes on Fuerteventura do not therefore
469	typically lead to the development of laterites and mature weathering profiles, since these conditions do not
470	favor the formation and subsequent preservation of these products, particularly within the carbonatite
471	bedrock areas. Consequently, this constraint substantially reduces the capacity of the FBC to potentially
472	contain economically valuable REE concentrations within the associated weathering products.
473	
474	5.3 Fuerteventura carbonatites as potential REE source
475	Based on the mineralogical and geochemical data, it can be concluded that, among the lithologies studied
476	in the FBC, only the carbonatites are favorable targets for further characterization and evaluation of their
477	potential economic viability as an REE source. Therefore, the primary alkaline rocks, as well as the entire
478	suite of corresponding secondary weathering products, can be ruled out.
479	The geochemical data obtained from the oceanic carbonatites of Fuerteventura, exemplified in multielement
480	and REE diagrams (Figure 8), suggest a petrogenetic affinity with carbonatites associated with
481	intracontinental rift geological settings. This similarity has also been previously highlighted by other
482	authors such as Carnevale et al. (2021) who, based on stable isotope data ($\delta^{13}C$ and $\delta^{18}C$) and noble gases
483	isotopic composition (He, Ne, Ar), suggested that oceanic and continental carbonatites were comparable in
484	petrogenetic terms. Therefore, despite the lingering questions about the formation processes of oceanic
485	carbonatites, their assessment as a possible source of critical metals, especially REEs, should be fully
486	considered in the same way as their continental counterparts.
487	However, when considering a more detailed assessment of the sectors where the FBC carbonatites outcrop,
488	it is essential to note that the distribution of these outcrops and thus potential REE mineralization is not
489	straightforward. The carbonatite outcrops have a very limited surface distribution, in the order of meters
490	(Figure 2e), and exhibit complex structural features influenced by shear metamorphism (Figure 2c) and
491	overlapping episodes of intrusive activity that resulted in swarms of dikes with intricate distributions (Figs.
492	2a, b). Hence, these general features of the carbonatite outcrops make it imperative to validly estimate their
493	volume and to carry out more precise studies of their depth distribution, which likely involve drilling and





494	geophysical	techniques. These prospective hypothetical findings would provide a deeper understanding of
495	the morpholo	ogy and dimensions of the carbonatitic bodies, enhancing the ability to calculate resources and
496	reserves whi	le refining the general metallogenic modeling.
497	However, it	is important to highlight that any attempt to assess potential REE deposits linked to FBC
498	carbonatites	must consider the possibility of regulatory constraints in the studied sectors. More specifically,
499	such constra	ints may stem from environmental considerations to safeguard natural and marine-coastal
500	areas, as we	Il as the allocation of land for strategic military activities. This latter point is particularly
501	pertinent for	a specific area within sector 3 (Figure 1). Therefore, any comprehensive analysis of the
502	potential of I	FBC carbonatites as REE sources must also factor in these potential restrictions tied to land use
503	regulations a	imed at upholding the broader socio-economic, environmental, and societal interests inherent
504	to a distinctiv	ve site like the island of Fuerteventura.
505		
506	6 Conclusio	ns
507	A preliminar	ry evaluation of rare earth element (REE) content was conducted through a mineralogical and
508	geochemical	study of alkaline and carbonatitic igneous rocks within the Fuerteventura basal complex
509	(FBC), along	g with associated weathering products. Based on the gathered data and their corresponding
510	interpretation	ns, our findings can be summarized as follows:
511	(i)	The concentrations of REEs present in the alkaline and carbonatitic rocks of the FBC are
512		significant and exceed the average values attributed to the Earth's crust.
513	(ii)	The weathering products developed on these magmatic rocks do not exhibit significant REE
514		enrichment. This aspect is particularly evident in the calcified horizons (Bk, calcretes), which
515		have practically negligible concentrations of these elements. Colluvial processes may have
516		influenced the lateral transport and accumulation of REEs in Pleistocene-Holocene deposits
517		distant from the source area.
518	(iii)	Among the magmatic rocks, carbonatites are the only lithology studied within the FBC with
519		a real potential to host REE mineral resources. The detected concentrations of REY in
520		carbonatites range up to 10,301.83 ppm, which is a comparable concentration to other
521		locations hosting significant deposits of these critical elements worldwide.
522	(iv)	Within carbonatites, REEs are primarily hosted in two accessory mineral phases: (1) oxides
523		belonging to the pyrochlore group; and (2) phosphates. In this second group, primary phases





524		such as REE-bearing britholite can be distinguished, as well as monazite generated as a
525		secondary product from the britholite alteration.
526	(v)	Primary calcite in the Fuerteventura carbonatites is not the predominant host of REEs. It
527		displays a highly homogeneous composition with insignificant Fe-Mg content and negligible
528		REEs.
529	(vi)	The carbonatites within the FBC could be considered potential REE resources associated with
530		a non-conventional geological setting. However, the complex structural features of the studied
531		FBC outcrops (deformation, metamorphism, swarms of dikes from different intrusive
532		pulses) make it essential to conduct more detailed studies to quantify the real economic
533		possibilities of this lithology as an REE source.
534	(vii)	All the studied sectors contain outcrops located in restricted areas due to environmental or
535		military use concerns. Any further detailed evaluation of the FBC carbonatites must take into
536		account the environmental, socio-economic, and geostrategic factors that will significantly
537		limit the real potential extension of REE deposits, considering a hypothetical exploitation.
538		
539	Acknowled	gements
540	This researe	ch was funded by the "Tierras Raras" project (SD-22/25) and the "MAGEC-REEmounts"
541	project (ProID-20211010027) of the Canarian Agency for Research, Innovation and Information Society	
542	(ACIISI by its initials in Spanish) of the Canary Islands Government. Funding support was also provided	
543	by the proj	ect "Materials for Advanced Energy Generation" (ENE2013-47826-C4-4-R), "3D Printed
544	Advanced M	Materials for Energy Applications" (ENE2016-74889-C4-2-R) and "Estudio de los procesos
545	magmáticos	s, tectónicos y sedimentarios involucrados en el crecimiento temprano de edificios volcánicos
546	oceánicos e	n ambiente de intraplaca" (CGL2016-75062-P), all funded by the Government of Spain. The
547	collection c	of samples in specific protected areas required authorization from the Fuerteventura Island
548	Governmen	t. We appreciate the cooperation and assistance provided by the Spanish Army, especially by
549	the soldier	Liberto Yeray Puga Acosta, who facilitated our access to the Pájara CMT restricted military
550	area to carry	y out sampling. We also thank Gerard Lucena from the LPGiP-MCNB for his thorough work in
551	the elaborat	ion of polished thin sections.

553 Statements and Declarations





554 Data availability statement

- 555 The authors confirm that the data supporting the findings of this study are available within the article and
- 556 its supplementary materials.
- 557

558 Competing interests

- 559 The authors declare no competing interests. The funders had no role in the design of the study, in the
- 560 collection of samples, the analyses, the interpretation of data, the writing of the manuscript nor the decision
- to publish these results.

562 Author contributions

- 563 Conceptualization: MC, IM, LQ, JY, JM; fieldwork and sampling: MC, IM, LQ, JY, RC, AA, JM;
- 564 methodology: MC, IM, JY, JM; validation of results: MC, IM, LQ, JY, RC, JMR, JM; data curation: MC,
- 565 IM, JM; writing-original draft preparation: MC, IM, JY, JM; writing-review editing: MC, IM, LQ, JY, RC,
- 566 JMR, JM; supervision: IM, JY, JM; project administration: JMR, JM; funding acquisition: IM, JY, RC,
- 567 JMR, JM.

568

569 Additional information

570 Supplementary tables are available in the online version at https: <u>XXXXX</u>





571 References

572	Acosta-Mora, P., Domen, K., Hisatomi, T., Lyu, H., Méndez-Ramos, J., Ruiz-Morales, J. C., Khaidukov,
573	N. M.: "A bridge over troubled gaps": up-conversion driven photocatalysis for hydrogen generation
574	and pollutant degradation by near-infrared excitation, Chem. Commun, 54, 1905 -1908
575	https://doi.org/10.1039/C7CC09774C, 2018.
576	Aiglsperger, T., Proenza, J. A., Lewis, J. F., Labrador, M., Svojtka, M., Rojas-Purón, A., Longo, F.,
577	Ďurišová, J.: Critical metals (REE, Sc, PGE) in Ni laterites from Cuba and the Dominican Republic,
578	Ore Geol. Rev., 73, 127-147, https://doi.org/10.1016/j.oregeorev.2015.10.010, 2016.
579	Ahijado, A.: Las intrusiones plutónicas e hipoabisales del sector meridional del Complejo Basal de
580	Fuerteventura, Doctoral Thesis, Universidad Complutense de Madrid, 392 p., 1999.
581	Ahijado, A., Casillas, R., Nagy, G., Fernández, C.: Sr-rich minerals in a carbonatite skarn, Fuerteventura,
582	Canary Islands (Spain), Mineralogy and Petrology, 84, 107-127, https://doi.org/10.1007/s00710-005-
583	<u>0074-8,</u> 2005.
584	Alonso, E., Sherman, A. M., Wallington, T. J., Everson, M. P., Field, F. R., Roth, R., Kirchain, R. E.:
585	Evaluating Rare Earth Element Availability: A Case with Revolutionary Demand from Clean
586	Technologies, Environ. Sci. Technol., 46, 3406–3414, https://doi.org/10.1021/es203518d, 2012.
587	Alonso-Zarza, A. M., Silva, P. G.: Quaternary laminar calcretes with bee nests evidences of small-scale
588	climatic fluctuations, Eastern Canary Islands, Spain, Palaeogeogr. Palaeoclimatol. Palaeoecol., 178,
589	119-135, https://doi.org/10.1016/S0031-0182(01)00405-9, 2002.
590	Alonso-Zarza, A. M., Rodríguez-Berriguete, Á., Casado, A. I., Martín-Pérez, A., Martín-García, R.,
591	Menéndez, I., Mangas, J.: Unravelling calcrete environmental controls in volcanic islands, Gran
592	Canaria Island, Spain, Palaeogeogr. Palaeoclimatol. Palaeoecol., 554, 109797,
593	https://doi.org/10.1016/j.palaeo.2020.109797, 2020.
594	Ancochea, E., Brändle, J. L., Cubas, C. R., Hernán, F., Huertas, M. J.: Volcanic complexes in the eastern
595	ridge of the Canary Islands: the Miocene activity of the Island of Fuerteventura, Journal of
596	Volcanology and Geothermal Research, 70, 183-204, <u>https://doi.org/10.1016/0377-0273(95)00051-</u>
597	<u>8</u> , 1996.
598	Ancochea, E., Barrera, J. L., Bellido, F.: Canarias y el vulcanismo neógeno peninsular. Geología de España,
599	635-682. In: Aparicio, A., Hernán, F., Cubas, C. R., Araña, V., 2003, Fuentes mantélicas y evolución
600	del volcanismo canario, Estudios Geológicos, 59, 5-13, https://doi.org/10.3989/egeol.03591-477,
601	2004.
602	Andersen, A. K., Clark, J. G., Larson, P. B., Donovan, J. J.: REE fractionation, mineral speciation, and
603	supergene enrichment of the Bear Lodge carbonatites, Wyoming, USA, Ore Geology Reviews, 89,
604	780-807, https://doi.org/10.1016/j. oregeorev.2017.06.025, 2017.
605	Balcells, R., Barrera, J. L., Gómez, J. A., Cueto, L. A., Ancochea, E., Huertas, M. J., Ibarrola, E., Snelling,
606	N.: Edades radiométricas en la Serie Miocena de Fuerteventura (Islas Canarias), Bol. Geol. Min., 35,
607	450–470, 1994.
608	Balaram, V.: Rare earth elements: A review of applications, occurrence, exploration, analysis, recycling,
609	and environmental impact, Geoscience Frontiers, 10, 1285-1303,
610	https://doi.org/10.1016/j.gsf.2018.12.005, 2019.





611	Balogh, K., Ahijado, A., Casillas, R., Fernández, C.: Contributions to the chronology of the Basal Complex
612	of Fuerteventura, Canary Islands, Journal of Volcanology and Geothermal Research, 90, 81-101,
613	https://doi.org/10.1016/S0377-0273(99)00008-6, 1999.
614	Bao, Z., Zhao, Z.: Geochemistry of mineralization with exchangeable REY in the weathering crusts of
615	granitic rocks in South China, Ore Geol. Rev., 33, 519-535,
616	https://doi.org/10.1016/j.oregeorev.2007.03.005, 2008.
617	Barrera, J. L., Fernández-Santín, S., Fúster, J. M., Ibarrola, E.: Ijolitas-Sienitas-Carbonatitas de los Macizos
618	del Norte de Fuerteventura, Bol. Geol. Min., TXCII-IV, 309-321. ISSN 0366-0176, 1993.
619	Barteková, E., Kemp, R., National strategies for securing a stable supply of rare earths in different world
620	regions, Resources Policy, 49, 153-164, https://doi.org/10.1016/j.resourpol.2016.05.003, 2016.
621	Beland, C. M. J., William-Jones, A. E.: The mineralogical distribution of the REE in carbonatites: A
622	quantitative evaluation, Chemical Geology, 585, 120558,
623	https://doi.org/10.1016/j.chemgeo.2021.120558, 2021.
624	Berger, A., Janots, E., Gnos, E., Frei, R., Bernier, F., Rare earth element mineralogy and geochemistry in
625	a laterite profile from Madagascar. Applied Geochemistry 41, 218-228,
626	https://doi.org/10.1016/j.apgeochem.2013.12.013, 2014.
627	Binnemans, K., Jones, P. T., Van Acker, K., Blanpain, B., Mishra, B., Apelian, D.: Rare-Earth Economics:
628	The Balance Problem, JOM, 65, 846-868, https://doi.org/10.1007/s11837-013-0639-7, 2013.
629	Borst, A. M., Smith, M. P., Finch, A. A., Estrade, G., Villanova-de-Benavent, C., Nason, P., Marquis, E.,
630	Horsburgh, N. J., Goodenough, K. M., Xu, C., Kynický, J., Geraki, K.: Adsorption of rare earth
631	elements in regolith-hosted clay deposits, Nat. Commun., 11, 4386, https://doi.org/10.1038/s41467-
632	<u>020-17801-5,</u> 2020.
633	Braga, J. M., Biondi, J. C.: Geology, geochemistry, and mineralogy of saprolite and regolith ores with Nb,
634	P, Ba, REEs (+ Fe) in mineral deposits from the Araxá alkali-carbonatitic complex, Minas Gerais
635	state, Brazil, Journal of South American Earth Sciences, 125, 104311,
636	https://doi.org/10.1016/j.jsames.2023.104311, 2023.
637	Braun, J. J., Pagel, M., Herbilln, A., Rosin, C.: Mobilization and redistribution of REEs and thorium in a
638	syenitic lateritic profile: A mass balance study, Geochem. Cosmochim. Acta, 57, 4419-4434.
639	https://doi.org/10.1016/0016-7037(93)90492-F, 1993.
640	Carnevale, G., Caracausi, A., Correale, A., Italiano, L., Rotolo, S.G., An Overview of the Geochemical
641	Characteristics of Oceanic Carbonatites: New Insights from Fuerteventura Carbonatites (Canary
642	Islands), Minerals, 11, 203. https://doi.org/10.3390/min11020203, 2021.
643	Casillas, R., Nagy, G., Demény, A., Ahijado, A., Fernández, C.: Cuspidine-niocalite-baghdadite solid
644	solutions in the metacarbonatites of the Basal Complex of Fuerteventura (Canary Islands). Lithos
645	105:25-41. https://doi.org/10.1016/j.lithos.2008.02.003, 2008.
646	Casillas, R., Démeny, A., Nagy, G., Ahijado, A., Fernández, C.: Metacarbonatites in the Basal Complex of
647	Fuerteventura (Canary Islands). The role of fluid/rock interactions during contact metamorphism and
648	anatexis, Lithos, 125, 503-520, https://doi.org/10.1016/j.lithos.2011.03.007, 2011.
649	Castor, S. B.: The Mountain Pass rare-earth carbonatite and associated ultrapotassic rocks, California, The
650	Canadian Mineralogist, 46, 779-806, https://doi.org/10.3749/canmin.46.4.779, 2008.





651	Chakhmouradian, A. R., Wall, F.: Rare Earth Elements: Minerals, Mines, Magnets (and More), Elements,
652	8, 333-340, https://doi.org/10.2113/gselements.8.5.333, 2012.
653	Chao, E. C. T., Back, J. M., Minkin, J. A., Tatsumoto, M., Wang, J., Conrad, J. E, McKee, E. H., Hou, Z.
654	L., Meng, Q. R., Huang, S. G.: The sedimentary carbonate-hosted giant Bayan Obo REE-Fe-Nb ore
655	deposit of Inner Mongolia, China: a corner stone example for giant polymetallic ore deposits of
656	hydrothermal origin, USGS Bulletin, 2143, 65, https://doi.org/10.3133/b2143, 1997.
657	Charalampides, G., Vatalis, K., Baklavaridis, A., Benetis, N. P.: Rare Earth Elements: Industrial
658	Applications and Economic Dependency of Europe, Procedia Economics and Finance, 24, 126-135,
659	https://doi.org/10.1016/S2212-5671(15)00630-9, 2015.
660	Chebotarev, D. A., Doroshkevich, A., Klemd, R., Karmanov, N.: Evolution of Nb- mineralization in the
661	Chuktukon carbonatite massif, Chadobets upland (Krasnoyarsk Territory, Russia), Periodico di
662	Mineralogia, 86, 99-118, https://doi.org/10.2451/2017PM733, 2017.
663	Chen, W., Honghui, H., Bai, T., Jiang, S.: Geochemistry of Monazite within Carbonatite Related REE
664	Deposits, Resources, 6, 51, https://doi.org/10.3390/resources6040051, 2017.
665	Chiquet, A., Michard, A., Nahon, D., Hamelin, B.: Atmospheric input vs in situ weathering in the genesis
666	of calcretes: an Sr isotope study at Gálvez (Central Spain), Geochim. Cosmochim. Acta, 63, 311-323,
667	https://doi.org/10.1016/S0016-7037(98)00271-3, 1999.
668	Christy, A. G., Atencio, D.: Clarification of status of species in the pyrochlore supergroup, Mineralogical
669	Magazine, 77, 13-20, https://doi.org/10.1180/minmag.2013.077.1.02, 2013.
670	Christy, A.G., Pekov, I.V., Krivovichev, S.G., The Distinctive Mineralogy of Carbonatites, Elements, 17,
671	333-338, https://doi.org/10.2138/gselements.17.5.333, 2021.
672	Coello, J., Cantagrel, J. M., Hernán, F., Fúster, J. M., Ibarrola, E., Ancochea, E., Casquet, C., Jamond, C.,
673	Díaz-de-Terán, J. R., Cendrero, A.: Evolution of the Eastern volcanic ridge of Canary Islands based
674	on new K-Ar data, Journal of Volcanology and Geothermal Research, 53, 251-274,
675	https://doi.org/10.1016/0377-0273(92)90085-R, 1992.
676	Connelly, N. G., Hartshorn, R. M., Damhus, T., Hutton, A. T.: Nomenclature of Inorganic Chemistry
677	IUPAC Recommendations 2005, RSC Publishing, Cambridge, ISBN-0-85404-438-8, 2005.
678	Courtillot, V., Davaille, A., Besse, J., Stock, J.: Three distinct types of hotspots in the Earth's mantle, Earth
679	Planet. Sci. Letters, 205, 295–308, https://doi.org/10.1016/S0012-821X(02)01048-8, 2003.
680	De Ignacio, C., Muñoz, M., Sagredo, J., Carbonatites and associated nephelinites from São Vicente, Cape
681	Verde Islands, Min., Mag., 76, 311-355, doi:10.1180/minmag.2012.076.2.05, 2012.
682	Demény, A., Ahijado, A., Casillas, R., Vennemann, T.W., Crustal contamination and fluid/rock interaction
683	in the carbonatites of Fuerteventura (Canary Islands, Spain): A C, O, H isotope study, Lithos, 44, 101-
684	115, https://doi.org/10.1016/S0024-4937(98)00050-4, 1998.
685	Dostal, J.: Rare Earth Element Deposits of Alkaline Igneous Rocks, Resources, 6, 34-46,
686	https://doi.org/10.3390/resources6030034, 2017.
687	Doucelance, R., Hammouda, T., Moreira, M., Martins, J.C., Geochemical constraints on depth of origin of
688	oceanic carbonatites: The Cape Verde case, Geochim. Cosmochim. Acta, 74, 7261-7282,
689	https://doi.org/10.1016/j.gca.2010.09.024, 2010.





690	Doucelance, R., Bellot, N., Boyet, M., Hammouda, T., Bosq, C., What coupled cerium and neodymium
691	isotopes tell us about the deep source of oceanic carbonatites, Earth Planet. Sci. Lett., 407, 175-186,
692	https://doi.org/10.1016/j.epsl.2014.09.042, 2014.
693	European Commission: European Green Deal, <u>https://commission.europa.eu/strategy-and-</u>
694	policy/priorities-2019-2024/european-green-deal_en, 2019.
695	European Commission: Study on the Critical Raw Materials for the EU 2023 - Final Report,
696	https://op.europa.eu/en/publication-detail/-/publication/57318397-fdd4-11ed-a05c-01aa75ed71a1 -
697	https://doi.org/10.32873/725585, 2023a.
698	European Commission, Regulation of the European Parliament and of the Council establishing a framework
699	for ensuring a secure and sustainable supply of critical raw materials and amending Regulations (EU)
700	168/2013, (EU) 2018/858, 2018/1724 and (EU) 2019/1020, https://eur-lex.europa.eu/legal-
701	content/EN/TXT/?uri=CELEX%3A52023PC0160, 2023b.
702	Falconnet, P.: The economics of rare earths, J. Less-Common Met., 111, 9-15,
703	https://doi.org/10.1016/0022-5088(85)90163-8, 1985.
704	FAO/UNESCO: Soil Map of the World Project 1:5000000, Chart VI1, https://www.fao.org/soils-
705	portal/data-hub/soil-maps-and-databases/faounesco-soil-map-of-the-world/en/, 1974.
706	Feraud, G., Giannerini, G., Campredon, R., Stillman, C.J.: Geochronology of some canarian dike swarms:
707	contribution to the volcano-tectonic evolution of the archipielago, J. Volcanol. Geotherm. Res., 25,
708	29-52, https://doi.org/10.1016/0377-0273(85)90003-4, 1985.
709	Fernández, C., Casillas, R., Ahijado, A., Perelló, V., Hernández-Pacheco, A.: Shear zones as a result of
710	intraplate tectonics in oceanic crust: the example of the Basal Complex of Fuerteventura (Canary
711	Islands), Jour. Struct. Geol., 19, 41-57, https://doi.org/10.1016/S0191-8141(96)00074-0, 1997.
712	Frisch, T.: In: Schmincke, H. U., Sumita, M.: Geological evolution of the Canary Islands: a young volcanic
713	archipelago adjacent to the old African continent, Bull Volcanol., 74, 1255-1256,
714	https://doi.org/10.1007/s00445-012-0605-1, 2012.
715	Fúster, J. M., Cendrero, A., Gastesi, P., Ibarrola, E., López-Ruiz, J.: Geología y volcanología de las Islas
716	Canarias- Fuerteventura, Instituto "Lucas Mallada", Consejo Superior de Investigaciones Científicas,
717	Madrid. 239 pp, 1968.
718	Goodenough, K. M., Schilling, J., Jonsson, E., Kalvig, P., Charles, N., Tuduri, J., Deady, E. A., Sadeghi,
719	M., Schiellerup, H., Müller, A., Bertrand, G., Arvanitidis, N., Eliopoulos, D. G., Shaw, R. A., Thrane,
720	K., Keulen, N.: Europe's rare earth element resource potential: An overview of REE metallogenetic
721	provinces and their geodynamic setting, Ore Geol. Rev., 72, 838-856,
722	https://doi.org/10.1016/j.oregeorev.2015.09.019, 2016.
723	Goudie, A. S., Middleton, N. J.: Saharan dust storms: nature and consequences, Earth Sci. Rev., 56, 179-
724	204, https://doi.org/10.1016/S0012-8252(01)00067-8, 2001.
725	Graedel, T. E., Harper, E. M., Nassar, N. T., Reck, B. K.: Criticality of metals and metalloids, Proceedings
726	of the National Academy of Sciences, 112 4257-4262, https://doi.org/10.1073/pnas.1500415112,
727	2015.
728	Gutiérrez, M., Casillas, R., Fernández, C., Balogh, K., Ahijado, A., Castillo, C., Colmenero, J. R., García-
729	Navarro, E.: The submarine volcanic succession of the basal complex of Fuerteventura, Canary





730	Islands: A model of submarine growth and emergence of tectonic volcanic islands, Bulletin of the
731	Geological Society of America, 118, 785-804, https://doi.org/10.1130/B25821.1, 2006.
732	Gutiérrez-Elorza, M., Lucha, P., Gracia, F. J., Desir, G., Marín, C., Petit-Maire, N.:_Palaeoclimatic
733	considerations of talus flatirons and aeolian deposits in Northern_Fuerteventura volcanic island
734	(Canary Islands, Spain), Geomorphology, 197, 1-9, https://doi.org/10.1016/j.geomorph.2011.09.020,
735	2013.
736	Haxel, G. B.: Ultrapotassic mafic dikes and rare earth element- and barium-rich carbonatite at Mountain
737	Pass, Mojave Desert, southern California: summary and field trip localities, U.S. Geol. Surv. Open-
738	File Rep., 1219. http://pubs.usgs.gov/of/2005/1219/, 2005.
739	Hobson, A., Bussy, F., Hernández, J.: Shallow-level migmatization of gabbrosin a metamorphic contact
740	aureole, Fuerteventura Basal Complex, Canary Islands, Journal of Petrology, 39, 1025-1037,
741	https://doi.org/10.1093/petroj/39.5.1025, 1998.
742	Hoernle, K., Tilton, G., Le Bas, M.J., Duggen, S., Garbe-Schönberg, D., Geochemistry of oceanic
743	carbonatites compared with continental carbonatites: Mantle recycling of oceanic crustal carbonate,
744	Contrib. Mineral. Petrol., 142, 520-542, https://doi.org/10.1007/s004100100308, 2002.
745	Holloway, M. I., Bussy, F.: Trace element distribution among rock-forming minerals from metamorphosed
746	to partially molten basic igneous rocks in a contact aureole (Fuerteventura, Canaries), Lithos, 102,
747	616-639, https://doi.org/10.1016/j.lithos.2007.07.026, 2008.
748	Huerta, P., Rodríguez-Berriguete, A., Martín-García, R., Martín-Pérez, A., La-Iglesia-Fernández, A.,
749	Alonso-Zarza, A.: The role of climate and eolian dust input in calcrete formation in volcanic islands
750	(Lanzarote and Fuerteventura, Spain), Palaeogeogr. Palaeoclimatol. Palaeoecol., 417, 66-79,
751	https://doi.org/10.1016/j.palaeo.2014.10.008, 2015.
752	Humphreys-Williams, E.R., Zahirovic, S.: Carbonatites and Global Tectonics, Elements, 17, 339-344,
753	https://doi.org/10.2138/gselements.17.5.339, 2021.
754	Jahn, R., Blume, H. P., Asio, V. B., Spaargaren, O., Schad, P.: Guidelines for soil description, FAO, Rome
755	97 p, https://www.fao.org/3/a0541e/a0541e.pdf, 2006.
756	Jyothi, R. K., Thenepalli, T., Ahn, J. W., Parhi, P. K., Chung, K. W., Lee, J. Y.: Review of rare earth
757	elements recovery from secondary resources for clean energy technologies: grand opportunities to
758	create wealth from waste, J. Clean. Prod., 267, 122048, https://doi.org/10.1016/j.jclepro.2020.122048,
759	2020.
760	Kamenetsky, V.S., Doroshkevich, A.G., Elliot, H.A.L., Zaitsev, A.N., Carbonatites: Contrasting, Complex,
761	and Controversial, Elements, 17, 307-314, https://doi.org/10.2138/gselements.17.5.307, 2021.
762	Kravchenko, S. M., Pokrovsky, B. G.: The Tomtor alkaline ultrabasic massif and related REE-Nb deposits,
763	northern Siberia, Economic Geology, 90, 676-689, https://doi.org/10.2113/gsecongeo.90.3.676,
764	1995.
765	Kravchenko, S. M., Czamanske, G., Fedorenko, V. A.: Geochemistry of carbonatites of the Tomtor massif,
766	Geochem. Int., 41, 545–558, ISSN: 0016-7029, 2003.
767	Lai, X., Yang, X., Santosh, M., Liu, Y., Ling, M.: New data of the Bayan Obo Fe-REE-Nb deposit, Inner
768	Mongolia: Implications for ore gènesis, Precambrian Research, 263, 108-122,
769	https://doi.org/10.1016/j.precamres.2015.03.013, 2015.





770	Le Bas, M. J.: The pyroxenite-ijolite-carbonatite intrusive igneous complexes of Fuerteventura, Canary
771	Islands, J. Geol. Soc. London, 138, 496, https://doi.org/10.1144/gsjgs.138.4.0493, 1981.
772	Le Bas, M. J, Rex, D. C., Stillman, C. J.: The early magmatic chronology of Fuerteventura, Geol. Mag.,
773	123, 287–298, https://doi.org/10.1017/S0016756800034762, 1986.
774	Le Maitre, R.W., Igneous Rocks: a Classification and Glossary of Terms, Cambridge University Press,
775	Cambridge, U.K, 2002.
776	Le Maitre, R. W., Streckeisen, A., Zanettin, B., Le Bas, M. J., Bonin, B., Bateman, P., Bellieni, G., Dudek,
777	A., Efremova, S., Keller, J., Lameyre, J., Sabine, P. A., Schmid, R., Sorensen, H., Woolley, A. R.:
778	Igneous Rocks: A Classification and Glossary of Terms, 2 nd Edition, Cambridge, UK, Cambridge
779	Univ. Press, ISBN: 9780521619486, 2005.
780	Liu, Y. L., Ling, M. X., Williams, I. S., Yang, X. Y., Wang, C. Y., Sun, W.: The formation of the giant
781	Bayan Obo REE-Nb-Fe deposit, North China, Mesoproterozoic carbonatite overprinted Paleozoic
782	dolomitization, Ore Geology Reviews, 92, 73-83, https://doi.org/10.1016/j.oregeorev.2017.11.011,
783	2018.
784	Long, K. R., Van Gosen, B. S., Foley, N. K., Cordier, D.: The principal rare earth elements deposits of the
785	United States: A summary of domestic deposits and a global perspective,
786	https://pubs.usgs.gov/sir/2010/5220/, 2010.
787	Longpré, M. A., Felpeto, A.: Historical volcanism in the Canary Islands; part 1: A review of precursory
788	and eruptive activity, eruption parameter estimates, and implications for hazard assessment, Journal
789	of Volcanology and Geothermal Research, 419, 107363,
790	https://doi.org/10.1016/j.jvolgeores.2021.107363, 2021.
791	Machado-Yanes, M. C.: Reconstrucción paleoecológica y etnoarqueológica por medio del análisis
792	antracológico.La Cueva de Villaverde, Fuerteventura, In: Biogeografía Pleistocena-Holocena de la
793	Península Ibérica, 261274, Ramil-Rego, P., Fernández-Rodríguez, C., Rodríguez-Guitián, M. (Eds.),
794	ISBN 84-453-1716-4, 261 p, 1996.
795	Mangas, J., Pérez-Torrado, F. J., Reguillón, R. M., Cabrera, M. C.: Prospección radiométrica en rocas
796	alcalinas y carbonatitas de la serie plutónica I de Fuerteventura (Islas Canarias). Resultados
797	preliminares e implicaciones metalogénicas, Actas del III Congreso Geológico de España y VIII
798	Congreso Latinoamericano de Geología. Salamanca, 3, 389–393, ISBN: 84-600-8114-1, 1992.
799	Mangas, J., Pérez-Torrado, F. J., Reguillón, R. M., Martin-Izard, A.: Mineralizaciones de tierras raras
800	ligadas a los complejos intrusivos alcalino-carbonatíticos de Fuerteventura (Islas Canarias), Bol. Soc.
801	Esp. Min., 17, 212–213, 1994.
802 803	Mangas, J., Pérez-Torrado, F. J., Reguillón, R. M., Martin-Izard, A.: Rare earth minerals in carbonatites of
803 804	Basal Complex of Fuerteventura (Canary Islands, Spain), In: Mineral Deposit: Research and Exploration, where do they meet? Ed. Balkema, Rotterdam, 475–478, ISBN-13: 978-9054108894,
804	
805	1997. Mariana A. N. Mariana Jr. A. Bara carth mining and exploration in North America. Flaments, 8, 260.
807	Mariano, A. N., Mariano, Jr. A.: Rare earth mining and exploration in North America, Elements, 8, 369–376, https://doi.org/10.2113/gselements.8.5.369, 2012.
808	Massari, S., Ruberti, M.: Rare earth elements as critical raw materials: Focus on international markets and
808	future strategies, Resour. Policy, 38, 36–43, <u>https://doi.org/10.1016/j.resourpol.2012.07.001</u> , 2013.
507	Tarate State Bross, resource roley, 50, 50 - 15, <u>maps.//doi.org/10.1010/j.icsourpol.2012.0/.001</u> , 2015.





810	McDonough, W., Sun, W.: The composition of the Earth, Chemical Geology, 67, 1050-1056,
811	https://doi.org/10.1016/0009-2541(94)00140-4, 1995.
812	McNulty, T., Hazen, N., Park, S., Processing the ores of rare-earth elements, MRS Bulletin, 47, 258-266,
813	https://doi.org/10.1557/s43577-022-00288-4, 2022.
814	Méndez-Ramos, J., Acosta-Mora, P., Ruiz-Morales, J. C., Hernández, T., Morge, M. E., Esparza, P.:
815	Turning into the blue: materials for enhancing TiO_2 photocatalysis by up-conversion photonics, RSC
816	Advances, 3, 23028–23034, https://doi.org/10.1039/C3RA44342F, 2013.
817	Menéndez, I., Díaz-Hernández, J. L., Mangas, J., Alonso, I., Sánchez-Soto, P. J.: Airborne dust
818	accumulation and soil development in the North-East sector of Gran Canaria (Canary Islands, Spain),
819	J. Arid Environ., 71, 57-81, <u>https://doi.org/10.1016/j.jaridenv.2007.03.011</u> , 2007.
820	Menéndez, I., Campeny, M., Quevedo-González, L., Mangas, J., Llovet, X., Tauler, E., Barrón, V., Torrent,
821	J., Méndez-Ramos, J.: Distribution of REE-bearing minerals in felsic magmatic rocks and paleosols
822	from Gran Canaria, Spain: Intraplate oceanic islands as a new example of potential, non-conventional
823	sources of rare-earth elements, Journal of Geochemical Exploration, 204, 270-288,
824	https://doi.org/10.1016/j.gexplo.2019.06.007, 2019.
825	Moore, M., Chakhmouradian, A., Mariano, A. N., Sidhu, R.: Evolution of Rare-earth Mineralization in the
826	Bear Lodge Carbonatite, In: Ore Geology Reviews, 64, Mineralogical and Isotopic Evidence,
827	Wyoming, 499, 521, http://dx.doi.org/10.1016/j.oregeorev.2014.03.015, 2015.
828	Mourão, C., Mata, J., Doucelance, R., Madeira, J., da Silveira, A.B., Silva, L.C., Moreira, M., Quaternary
829	extrusive calciocarbonatite volcanism on Brava Island (Cape Verde): A nephelinite-carbonatite
830	immiscibility product, Journal of African Earth Sciences, 56, 59-74,
831	https://doi.org/10.1016/j.jafrearsci.2009.06.003, 2010.
832	Muñoz, M.: Ring complexes of Pájara in Fuerteventura Island, Bulletin Volcanologique, 33, 840-861,
833	https://doi.org/10.1007/BF02596753, 1969.
834	Muñoz, M., Sagredo, J., de Ignacio, C., Fernández-Suárez, J., Jeffries, T. E.: New data (U-Pb, K-Ar) on the
835	geochronology of the alkaline-carbonatitic association of Fuerteventura, Canary Islands, Spain,
836	Lithos, 85, 140-153, https://doi.org/10.1016/j.lithos.2005.03.024, 2005.
837	Olson, J.C., Shawe, D. R., Pray, L.C., Sharp, W. N.: Rare-Earth Mineral Deposits of the Mountain Pass
838	District, San Bernardino County, California, Science, 119, 325-326,
839	https://doi.org/10.1126/science.119.3088.325, 1954.
~	<u>nups://doi.org/10.1120/science.119.5088.525</u> , 1954.
840	Park, J., Rye, D.M., Broader Impacts of the Metasomatic Underplating Hypothesis, Geochem. Geophys.
840 841	
	Park, J., Rye, D.M., Broader Impacts of the Metasomatic Underplating Hypothesis, Geochem. Geophys.
841	Park, J., Rye, D.M., Broader Impacts of the Metasomatic Underplating Hypothesis, Geochem. Geophys. Geosyst., 20, 4180–4829, https://doi.org/10.1029/2019GC008493, 2019.
841 842	 Park, J., Rye, D.M., Broader Impacts of the Metasomatic Underplating Hypothesis, Geochem. Geophys. Geosyst., 20, 4180–4829, https://doi.org/10.1029/2019GC008493, 2019. Pérez-Torrado, F. J., Carracedo, J. C., Guillou, H., Rodríguez-González, A., Fernández-Turiel, J. L.: Age,
841 842 843	 Park, J., Rye, D.M., Broader Impacts of the Metasomatic Underplating Hypothesis, Geochem. Geophys. Geosyst., 20, 4180–4829, https://doi.org/10.1029/2019GC008493, 2019. Pérez-Torrado, F. J., Carracedo, J. C., Guillou, H., Rodríguez-González, A., Fernández-Turiel, J. L.: Age, duration, and spatial distribution of ocean shields and rejuvenated volcanism: Fuerteventura and
841 842 843 844	 Park, J., Rye, D.M., Broader Impacts of the Metasomatic Underplating Hypothesis, Geochem. Geophys. Geosyst., 20, 4180–4829, https://doi.org/10.1029/2019GC008493, 2019. Pérez-Torrado, F. J., Carracedo, J. C., Guillou, H., Rodríguez-González, A., Fernández-Turiel, J. L.: Age, duration, and spatial distribution of ocean shields and rejuvenated volcanism: Fuerteventura and Lanzarote, Eastern Canaries, Journal of the Geological Society of London, 180,





848	Reinhardt, N., Proenza, J., Villanova-de-Benavent, C., Aiglsperger, T., Bover-Arnal, T., Torró, L., Salas,
849	R., Dziggel, A.: Geochemistry and Mineralogy of Rare Earth Elements (REE) in Bauxitic Ores of the
850	Catalan Coastal Range, NE Spain, Minerals, 8, 562, https://doi.org/10.3390/min8120562, 2018.
851	Scheuvens, D., Schütz, L., Kandler, K., Ebert, M., Weinbruch, S.: Bulk composition of northern African
852	dust and its source sediments-a compilation, Earth Sci. Rev., 116, 170-194,
853	https://doi.org/10.1016/j.earscirev.2012.08.005, 2013.
854	Schmincke, H., Sumita, M.: Geological evolution of the Canary Islands: a young volcanic archipelago adjacent
855	to the old African Continent, Ed. Görres, Koblenz, 200 p, ISBN: 978-3-86972-005-0, 2010.
856	Smith, M. P., Campbell, L. S., Kynicky, J.: A review of the genesis of the world class Bayan Obo Fe-REE-Nb
857	deposits, Inner Mongolia, China: multistage processes and outstanding qüestions, Ore Geology Reviews,
858	64, 459-476, https://doi.org/10.1016/j.oregeorev.2014.03.007, 2015.
859	Smith, M. P., Moore, K., Kavecsánszki, D., Finch, A. A., Kynicky, J., Wall, F.: From mantle to critical zone:
860	A review of large and giant-sized deposits of the rare earth elements, Geoscience Frontiers, 7, 315-334,
861	https://doi.org/10.1016/j.gsf.2015.12.006, 2016.
862	Steiner, C., Hobson, A., Favre, P., Stampli, G. M.: Early Jurassic sea-floor spreading in the central Atlantic
863	- the Jurassic sequence of Fuerteventura (Canary Islands), Geological Society of American Bulletin,
864	110, 1304-1317, https://doi.org/10.1130/0016-7606(1998)110<1304:MSOFCI>2.3.CO;2, 1998.
865	Torró, L., Proenza, J. A., Aiglsperger, T., Bover-Arnal, T., Villanova-de-Benavent, C., Rodríguez-García,
866	D., Ramírez, A., Rodríguez, J., Mosquea, L.A., Salas, R.: Geological, geochemical and mineralogical
867	characteristics of REE-bearing Las Mercedes bauxite deposit, Dominican Republic, Ore Geol. Rev.,
868	89, 114–131, https://doi.org/10.1016/j.oregeorev.2017.06.017, 2017.
869	Torró, L., Villanova, C., Castillo, M., Campeny, M., Gonçalves, A. O., Melgarejo, J. C.: Niobium and rare
870	earth minerals from the Virulundo carbonatite, Namibe, Angola, Mineralogical Magazine, 76, 393-
871	409, https://doi.org/10.1180/minmag.2012.076.2.08, 2012.
872	Troll, V., Carracedo, J. C.: The Geology of Fuerteventura, In: Troll, V., Carracedo, J. C., Weismaier, S.
873	(eds), The Geology of Canary Islands, Elsevier, 531-582. http://dx.doi.org/10.1016/B978-0-12-
874	<u>809663-5.00008-6</u> , 2016.
875	van den Bogaard, P.: The origin of the Canary Island Seamount Province - New ages of old seamounts,
876	Scientific Reports, 3, 2107. https://doi.org/10.1038/srep02107, 2013.
877	Wang, Q., Deng, J., Liu, X., Zhang, Q., Sun, S., Jiang, C., Zhou, F.: Discovery of the REE minerals and its
878	geological significance in the Quyang bauxite deposit, West Guangxi, China, J. Asian Earth Sci., 39,
879	701-712, https://doi.org/10.1016/j.jseaes.2010.05.005, 2010.
880	Wang, X., Jiao, Y., Du, Y., Ling, W., Wu, L., Cui, T., Zhou, Q., Jin, Z., Lei, Z., Wen, S.: REE mobility
881	and Ce anomaly in bauxite deposit of WZD area, Northern Guizhou, China, J. Geochem Explor., 133,
882	103–117, <u>https://doi.org/10.1016/j.gexplo.2013.08.009</u> , 2013.
883	Wang, Z.Y., Fan, H.R., Zhou, L., Yang, K.F., She, H.D., Carbonatite-related REE deposits: An
884	overview, Minerals, 10, 965. https://doi.org/10.3390/min10110965, 2020.
885	Warr, L. N.: IMA-CNMNC approved mineral symbols, Mineralogical Magazine, 85, 291-
886	320, https://doi.org/10.1180/mgm.2021.43, 2021.

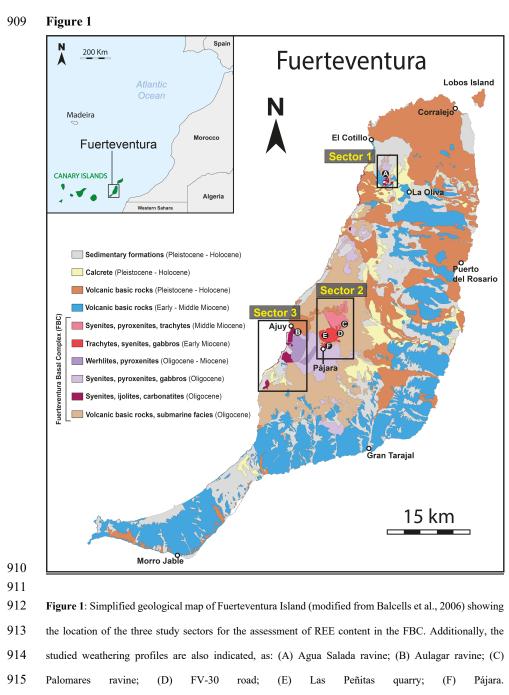




887	Weng, Z., Jowitt, S.M., Mudd, G.M., Haque, N.: A Detailed Assessment of Global Rare Earth Element
888	Resources: Opportunities and Challenges, Economic Geology, 110, 1925-1952,
889	https://doi.org/10.2113/econgeo.110.8.192, 2015.
890	Wondraczek, L., Tyystjärvi, E., Méndez-Ramos, J., Müller, F. A., Zhang. Q.: Shifting the Sun: Solar
891	Spectral Conversion and Extrinsic Sensitization in Natural and Artificial Photosynthesis, Advanced
892	Science, 2, 1500218, https://doi.org/10.1002/advs.201500218, 2015.
893	Woolley, A.R., Kjarsgaard, B.A. (2008): Carbonatites of the world: map and database. Mineralogical
894	Magazine 71, 718.
895	Wu, C.: Bayan Obo Controversy: Carbonatites versus Iron Oxide-Cu-Au-(REE-U), Resource Geology, 58,
896	348-354, https://doi.org/10.1111/j.1751-3928.2008.00069.x, 2008.
897	Yang, K., Fan, H., Pirajno, F., Li, X.: The bayan Obo (China) giant REE accumulation conundrum
898	elucidated by intense magmatic differentiation of carbonatite, Geology, 47, 1198-1202,
899	https://doi.org/10.1130/G46674.1, 2019.
900	Zazo, C., Goy, J. L., Hillaire-Marcel, C., Gillot, P. Y., Soler, V., González, J. A., Dabrio, C. J., Ghaleb, B.:
901	Raised marine sequences of Lanzarote and Fuerteventura revisited -a reappraisal of relative sea-level
902	changes and vertical movements in the eastern Canary Islands during the Quaternary, Quaternary
903	Science Reviews, 21, 2019–2046, https://doi.org/10.1016/S0277-3791(02)00009-4, 2002.
904	Zhukova, I. A., Stepanov, A. S., Jiang, S. Y., Murphy, D., Mavrogenes, J., Allen, C., Chen, W., Bottrill,
905	R.: Complex REE systematics of carbonatites and weathering products from uniquely rich Mount
906	Weld REE deposit, Western Australia, Ore Geology Reviews, 139, 104539,
907	https://doi.org/10.1016/j.oregeorev.2021.104539,2021.
908	







- 916
- 917
- 918





919 Figure 2



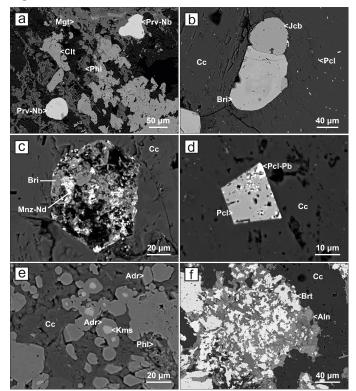
920

921 Figure 2: (a), (b) Images showing typical outcrops of the FBC in the southern area of Ajuy (sector 3; 922 Figure 1). The images highlight characteristic swarms of alkaline and carbonatitic intrusions (whitish) 923 intersected by later-intruded basaltic dikes (black colour). (c) Detailed view of a carbonatitic dike located 924 in a shear zone of sector 3, exhibiting distinct linear sigmoidal structures resulting from deformation. (d) 925 Detailed view of centimetre-sized phlogopite crystals within a carbonatitic dike outcropping in sector 3, 926 displaying a typical pegmatitic texture. (e) Overview of an outcrop of metric-scale carbonatitic dikes in the 927 sector 1 area.





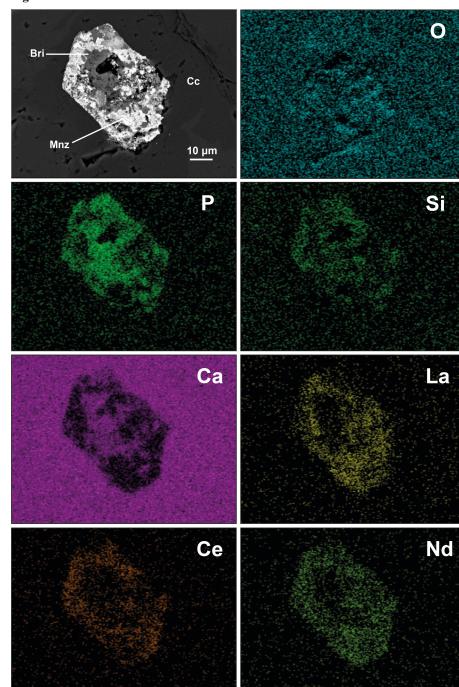




930 Figure 3: SEM (backscattered electron, BSE) images of the Fuerteventura carbonatites. (a) Subhedral 931 crystals of niobium-rich perovskite (Prv-Nb) associated with phlogopite (Phl) and magnetite (Mgt) 932 aggregates. The association has been affected by secondary hydrothermal processes, leading to the 933 formation of celestine (Clt). (b) Typical subhedral crystal of jacobsite (Jcb) associated with britholite (Bri). 934 Both crystals are hosted in magmatic calcite (Cc), with numerous disseminated microcrystals of pyrochlore 935 (Pcl). (c) Partially altered subhedral grain of britholite (Bri) hosted in magmatic calcite (Cc). The alteration 936 process led to the formation of secondary REE phosphates such as monazite-Nd (Mnz-Nd). (d) Euhedral 937 crystal of pyrochlore (Pcl) hosted in calcite (Cc). Brighter areas developed on the grain's borders correspond 938 to plumbopyrochlore (Pcl-Pb) zonation. (e) Typical mineral association related to small skarn like areas 939 associated with carbonatites. Subhedral zoned crystals of andradite (Adr), hosted in calcite (Cc) and 940 phlogopite (Phl), with a significant Zr zoning leading to kerimasite (Kms) cores. (f) Typical low-941 metamorphic alteration developed on carbonatites composed of allanite (Aln) aggregates hosted in calcite 942 (Cc) and associated with secondary baryte (Brt). Abbreviations of mineral names in all the pictures follow 943 the criteria proposed by Warr (2021).







944 Figure 4





947 of britholite (Bri) hosted in calcite (Cc) and partially transformed into secondary monazite (Mnz).

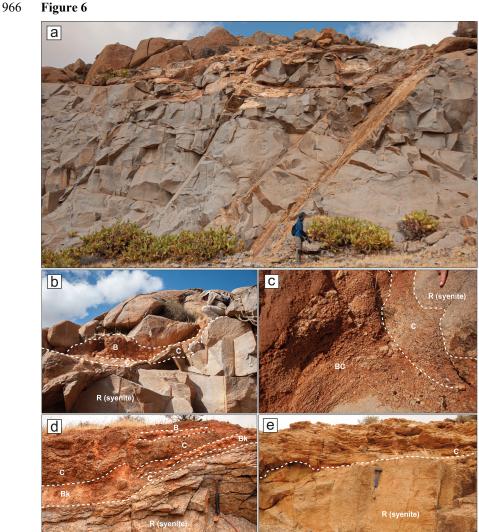




- Figure 5 ล Calcrete С Calcrete Figure 5: (a) General view of a typical surface outcrop of Quaternary calcrete located in the Aulagar ravine area (profile B, sector 3; Fig.1). (b) Centimetre-thick calcrete layer filling a fracture between two carbonatitic dikes in the Aulagar ravine area (profile B, sector 3; Fig.1). (c) Calcrete layer developed within fractures between carbonatitic rocks in the Agua Salada ravine area (profile A, sector 1; Fig.1).







967

968 Figure 6: (a) General view of Las Peñitas quarry syenite outcrop (profile E, sector 2; Fig.1) where it is 969 possible to distinguish different fractures filled by injected secondary weathering products. (b) Syenite 970 weathering profile in Las Peñitas quarry (profile E, sector 2; Figure 1) showing surface erosion and B, BC 971 and C horizons injected in the syenite bedrock (R). (c) Weathering profile displaying the development of 972 C and BC horizons associated with a syenite protolith (R), located in Las Peñitas quarry (profile E, sector 973 2; Figure 1). (d) Weathering profile developed on syenite in the FV-30 road area (profile D, sector 2), 974 exhibiting the development of C, B and calcrete (Bk) horizons. (e) Weathering profile on syenite protolith 975 (R) displaying a metric sized C horizon in the Pájara area (profile F, sector 2; Figure 1).





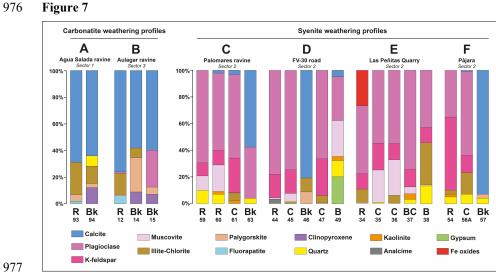
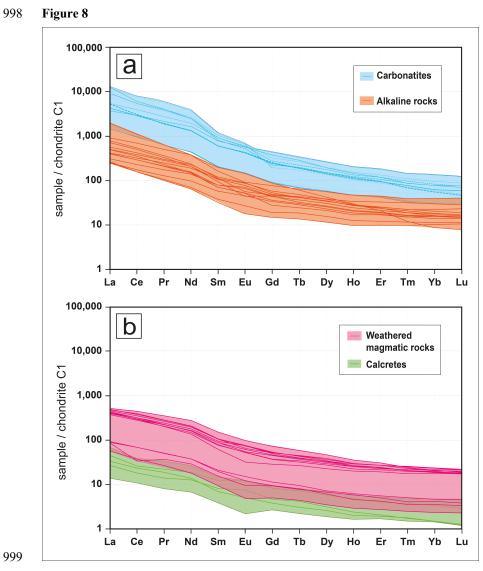
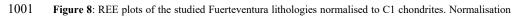


Figure 7: Graphical mineralogical quantification of the studied weathering profiles: (A) Agua Salada ravine; (B) Aulagar ravine; (C) Palomares ravine; (D) FV-30 road; (E) Las Peñitas quarry; (F) Pájara. The corresponding class assigned to the edaphic horizons (B, BC, Bk, C, R) and the sample number are shown at the foot of the columns.





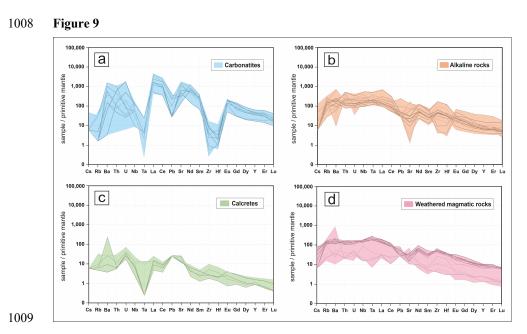




¹⁰⁰² values are from McDonough and Sun (1995).





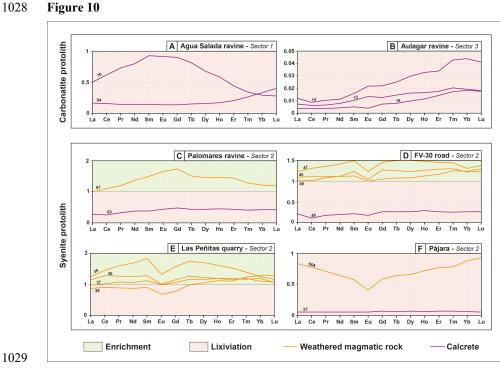


1010 Figure 9: Multi-elemental trace element plots of Fuerteventura intrusive lithologies normalised to the

1011 primitive mantle. Normalisation values from McDonough and Sun (1995).





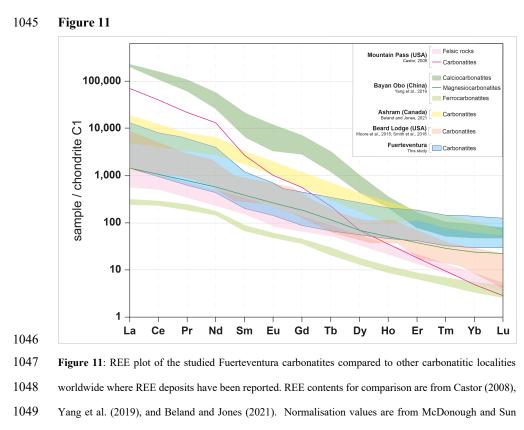


1030 Figure 10: REE weathering enrichment/leaching diagrams between primary magmatic protoliths1031 (carbonatites and syenites) and the associated weathering products from the studied profiles (Figure 1). The

1032 sample number is labelled on the corresponding pattern line.







1050 (1995).